

# Preparation, characterization, and in vivo pharmacokinetics of nanostructured lipid carriers loaded with oleanolic acid and gentiopicrodin

Kunchi Zhang

Shaowa Lv

Xiuyan Li

Yufei Feng

Xin Li

Lu Liu

Shuang Li

Yongji Li

School of Pharmacy, Heilongjiang University of Traditional Chinese Medicine, Harbin, Heilongjiang Province, People's Republic of China

**Background:** The purpose of this work was to develop nanostructured lipid carriers (NLCs) loaded simultaneously with oleanolic acid and gentiopicrodin.

**Methods:** An aqueous dispersion of NLCs was prepared successfully using a film-ultrasonic method, with glycerin monostearate as the solid lipid and oleic acid as the liquid lipid. Poloxamer 188 was used as the surfactant. A central composite design was used to optimize the technologic parameters. The characteristics of the NLCs were then investigated.

**Results:** The encapsulation efficiency was  $48.34\% \pm 2.76\%$ , drug loading was  $8.06\% \pm 0.42\%$ , particle size was  $111.0 \pm 1.56$  nm, polydispersity index was  $0.287 \pm 0.01$ , and zeta potential was  $-23.8 \pm 0.36$  mV for the optimized NLCs. The other physicochemical properties were characterized by transmission electron microscopy and differential scanning calorimetry. Drug release followed first-order kinetics and release studies confirmed that oleanolic acid and gentiopicrodin fitted a sustained-release model. Compared with NLCs loaded with oleanolic acid or gentiopicrodin alone, NLCs loaded with both oleanolic acid and gentiopicrodin produced drug concentrations which persisted for a significantly longer time in plasma, with a linear decrement following second-order kinetics. Aspartate and alanine aminotransferase levels were significantly lower on exposure to NLCs loaded with both oleanolic acid and gentiopicrodin than in negative controls.

**Conclusion:** The results of this study confirm that oleanolic acid and gentiopicrodin can be loaded simultaneously into NLCs. Compared with oleanolic acid and gentiopicrodin loaded alone, sustained release and protective effects against hepatic injury were observed using NLCs loaded with both oleanolic acid and gentiopicrodin.

**Keywords:** nanostructured lipid carriers, central composite design, in vitro release, pharmacokinetics

## Introduction

Gentian is a plant with clear and unique therapeutic effects in liver disease. The main active constituents of gentian are iridoids, in particular, gentiopicrodin. Kondo et al reported that gentiopicrodin has a protective effect against the acute hepatic damage caused by carbon tetrachloride and cures hepatitis B.<sup>1</sup> However, the half-life of gentiopicrodin is short, and its therapeutic effects are limited in its conventional form. It is generally believed that the acute hepatic damage caused by carbon tetrachloride arises from hepatic cellular necrosis due to changes in membrane fluidity and protein structure caused by lipid peroxidation.<sup>2</sup> Oleanolic acid is also a component of gentian, and has been used successfully to treat liver disease. In a study reported by Jeong, oleanolic acid had an inhibitory effect on lipid peroxidation.<sup>3</sup> However, because of its strong hydrophobicity, the therapeutic effects of oleanolic acid might

Correspondence: Yongji Li  
Heilongjiang University of Traditional Chinese Medicine, Heping Road 24, Harbin, People's Republic of China  
Tel +86 0451 8726 7038  
Fax +86 0451 8726 7038  
Email kunchizhang@163.com

not be satisfactory *in vivo*. Further, the dissolution rate of oleanolic acid is low, so its bioavailability and biological activity is limited.

One strategy for overcoming the rapid elimination of gentiopiricin and increasing the *in vivo* efficacy of oleanolic acid is to encapsulate these agents in nanoparticles, thereby changing their *in vivo* release characteristics and increasing their therapeutic effects.<sup>4</sup> A recent study demonstrated that nanostructured lipid carriers (NLCs) could be used to encapsulate both hydrophilic and hydrophobic drugs.<sup>5</sup> Lipid molecules in different phases (ie, liquid and solid) are mixed to create a lipid particle matrix that is as imperfect as possible. Because of the many imperfections in NLCs, drug-loading capacity is enhanced and the risk of drug expulsion during storage is minimized.<sup>6</sup> In the present study, NLCs were used as a carrier to entrap gentiopiricin and oleanolic acid in an effort to overcome the shortcomings of gentiopiricin and oleanolic acid used alone.

Over the last two decades, NLCs have been shown to have several advantages, ie, achievement of a higher solid content using NLC dispersions, better drug-loading capacity, and easily modulated drug release.<sup>7</sup> For these reasons, NLCs are used widely in drug delivery systems. Most of the current research is focused on loading of single drugs into NLCs.<sup>8–12</sup> However, in this study, we undertook the challenging task of preparing NLCs with balanced entrapment efficiency using gentiopiricin and oleanolic acid, the properties of which differ widely. Commonly used surfactants include Span, Tween, polyvinylpyrrolidone, and Poloxamer,<sup>13</sup> and NLCs can be prepared using a variety of methods, including high pressure homogenization, microemulsions, solvent dispersal, and film-ultrasonic methods.<sup>14</sup> In view of the properties of gentiopiricin and oleanolic acid and the preliminary nature of our experiments, the film-ultrasonic method was used in this study.

The literature indicates that nanoparticles in the size range of 100–150 nm can be passively targeted towards and accumulate in hepatic tissue.<sup>15</sup> Therefore, nanoparticles in the relatively small size range of 100–150 nm are desirable when targeting agents to the liver. The main aim of this study was to achieve optimal incorporation of gentiopiricin and oleanolic acid in NLCs using a film-ultrasonic method to enhance entrapment efficiency and a central composite design for the response surface. Suitably sized NLCs with high entrapment efficiency were successfully produced in an optimized formulation. Their physicochemical characteristics were also evaluated, along with their pharmacokinetic profiles *in vivo*.

## Materials and methods

### Materials

Gentiopiricin and oleanolic acid were obtained from ChengDu XHHC Biotechnology Co, Ltd (Ch'engtu, People's Republic of China). Single stearic acid glycerides was purchased from Aladdin Chemical Co, Ltd (Shanghai, People's Republic of China). Oleic acid was sourced from Jingchun Reagents Co, Ltd (Shanghai, People's Republic of China) and Poloxamer 188 from Yunhong Technology of Chemical Reagents Co, Ltd (Shanghai, People's Republic of China). Sephadex G-50 was supplied by Haoran Biotechnology Co, Ltd (Shanghai, People's Republic of China) and an enzyme-linked immunosorbent assay (ELISA) kit by Jijing Chemical Co., Ltd., (Shanghai, People's Republic of China). All high-performance liquid chromatography (HPLC) reagents were chromatographically pure and obtained from Dikma Technologies Inc (Lake Forest, CA, USA). The other chemicals used were purchased from Tianli Chemical Reagents Co, Ltd (Tianjin, People's Republic of China).

### Animals

The experiments were performed on healthy Sprague-Dawley rats (mean weight  $220 \pm 25$  g, mean age 10 weeks) and Kunming mice (mean weight  $20 \pm 5$  g), according to the current national legislation for animal experiments. Half of the animals were female and half were male, and all were randomized to the different treatment groups. All animals used were provided by the Experimental Animals Center, Heilongjiang University of Chinese Medicine, People's Republic of China.

### Methods

#### Preparation of GO-NLCs

NLCs loaded with both oleanolic acid and gentiopiricin (GO-NLCs) were prepared using an established film-ultrasonic method.<sup>16</sup> In brief, an aqueous phase was created by dissolving Poloxamer 188 in pure water and keeping it in a water bath at  $50^\circ\text{C} \pm 1^\circ\text{C}$ . The oil phase comprised mainly oleic acid, gentiopiricin, and oleanolic acid, which were melted in absolute ethyl alcohol whilst being stirred at a constant temperature using a magnetic stirrer (85-2A, Jintan Medical Instrument Factory, Jiangsu, People's Republic of China). The organic solvent was removed at  $45^\circ\text{C}$  under vacuum using a rotary evaporator (EYELA, Ailang Instrument Co., Ltd., Tianjin, People's Republic of China). Oil phase was dissolved in aqueous phase by ultrasonic dispersion using an ultrasonic cell pulverizer (VCX750, Sonics and Materials, Inc., Newtown, CA, USA) at the same temperature. The hot emulsion was then cooled to room temperature, and GO-NLCs were obtained.

## Central composite design of NLCs

In this study, a central composite design was used to optimize the GO-NLCs. After the most important factors influencing physicochemical characteristics had been investigated, the amounts of oleanolic acid, gentiopicrin, and oleic acid were selected as independent variables. Each factor was set at five levels, ie, +1, -1, 0, +a, and -a. The actual and coded values for the different variables are shown in Table 1. Fifteen formulations of NLCs were devised to optimize the experimental parameters, as shown in Table 2. The entrapment efficiencies of oleanolic acid encapsulated alone, gentiopicrin encapsulated alone, and oleanolic acid and gentiopicrin encapsulated simultaneously were used as a response parameter.

## Particle size, polydispersity index, and zeta potential

The particle size and zeta potential of the NLCs were measured using a Malvern Zetasizer 3000 (Malvern, Worcestershire, UK). The polydispersity index was used to quantify the particle size distribution. The NLCs were diluted prior to determination of particle size and zeta potential.<sup>17</sup>

## Entrapment efficiency and drug loading

The free drugs were separated from the GO-NLCs using Sephadex G-50 gel for measurement of entrapment efficiency. GO-NLCs were added into a Sephadex G-50 gel column and eluted with distilled water, followed by separation of the nanoparticles and free drugs. The free drugs were collected and their concentrations were determined by HPLC. The percent entrapment efficiency of GO-NLCs was calculated using equation (1) and percent drug loading of GO-NLCs was calculated using equation (2).<sup>18</sup>

$$EE\% = W - W1/W \times 100\% \quad (1)$$

$$DL\% = W - W1/WP \times 100\% \quad (2)$$

where EE% is percent entrapment efficiency, DL% is percent drug loading, W is the amount of drug added to the system, W1 is the amount of free drug in the system, and WP is the quality of the total carrier material.

**Table 1** Actual values of independent variables

	Name	Units	-1	1	-a	+a	0
X <sub>1</sub>	Oleanolic acid	mg	2	4	1	5	3
X <sub>2</sub>	Gentiopicrin	mg	2	4	1	5	3
X <sub>3</sub>	Oleic acid	mL	1.19	1.53	1.02	1.7	1.36

**Table 2** Formulations of nanostructured lipid carriers loaded with both oleanolic acid and gentiopicrin by central composite design

Run	X1	X2	X3	Response 1	Response 2	Response 3
F1	-a	0	0	Oleanolic acid EE (%)	Gentiopicrin EE (%)	Total EE (%)
F2	1	-1	-1			
F3	0	0	0			
F4	0	-a	0			
F5	-1	-1	-1			
F6	-1	1	1			
F7	-1	-1	1			
F8	0	0	a			
F9	0	0	-a			
F10	a	0	0			
F11	0	a	0			
F12	1	1	1			
F13	-1	1	-1			
F14	1	1	-1			
F15	1	-1	1			

**Abbreviation:** EE, entrapment efficiency.

## Transmission electron microscopy

The morphology of the GO-NLCs were observed using a transmission electron microscope (model TECNAIG2, Philips, Eindhoven, The Netherlands).<sup>19</sup> The GO-NLCs were then diluted 1:5 times and placed on copper grids with 2% (w/v) phosphotungstic acid staining for 40 seconds before further analysis.

## Differential scanning calorimetry

The physical state of the gentiopicrin and oleanolic acid loaded into the GO-NLCs was investigated by differential scanning calorimetry (Kisijia Instrument Company, Beijing, People's Republic of China) with a sampling interval of 1000 msec. Next, a 6 mg sample of freeze-dried NLC was heated from 0°C to 500°C at a rate of 10°C per minute. Glycerin monostearate, gentiopicrin, and oleanolic acid were also placed in the copper pan as controls.

## In vitro release

In vitro studies of the release of gentiopicrin and oleanolic acid from GO-NLCs were carried out using dialysis bags (Sigma, St Louis, MO, USA) soaked in double-distilled water for 12 hours before use. Freeze-dried GO-NLC suspensions not containing free drugs (removed using a Sephadex column) were put into a dialysis bag which was then placed in 50 mL of 20% ethanol in phosphate-buffered solution (pH 7.4) to maintain sink conditions and shaken at 100 rpm in a constant-temperature shaker (SHAB, Donglian Electric Technique Co. Ltd., Haerbin, People's Republic of China) at 37°C. Subsequently, 2 mL

of release medium was withdrawn at regular time intervals and fresh release medium was added to maintain a constant volume.<sup>20</sup> The samples were then analyzed by HPLC. Control experiments were performed in the same way using the same proportions of gentiopicrin and oleanolic acid as in the GO-NLCs to investigate drug release behavior.

## Pharmacokinetic studies

Thirty Sprague-Dawley rats were randomized into three groups to receive either GO-NLCs, NLCs loaded with gentiopicrin and normal saline, or NLCs loaded with oleanolic acid and normal saline. All rats were fasted for 12 hours before the experiments but had free access to water. A 10 mg/kg dose of the trial substance was injected via the caudal vein. Blood samples were collected in heparinized tubes at 10, 15, 30, 45, 60, 90, 120, 180, 240, and 360 minutes. Plasma was isolated from whole blood by centrifugation at 3000 rpm for 10 minutes. Next, 100  $\mu$ L of the separated plasma was spun with triple methanol in a centrifuge tube for 30 seconds and centrifuged at 10,000 rpm for five minutes. The supernatant was dried under nitrogen at 50°C, and 300  $\mu$ L of methanol was then added. The treated plasma was spun for one minute, and then filtered.<sup>21</sup> Finally, 10  $\mu$ L samples of plasma were injected into the HPLC column and the concentrations of gentiopicrin and oleanolic acid were determined. Pharmacokinetic parameters and the concentration time curve were analyzed using the 3P97 Pharmacokinetic program recommended by the Chinese Pharmacologic Association.

## Analysis of gentiopicrin and oleanolic acid by HPLC

Samples were analyzed using a photodiode array detector (Model 2996, Waters, Milford, MA, USA) and an HPLC column (C18, 4.6 mm  $\times$  250 mm, 5  $\mu$ m, Diamonsil Company, New York, NY, USA). The mobile phase for gentiopicrin was a mixture of methanol and water at a ratio of 50:50 (v/v) and for oleanolic acid was a mixture of methanol and water at a ratio of 90:10 (v/v). A detection wavelength of 270 nm was used for gentiopicrin and 210 nm for oleanolic acid. The flow rate was 1 mL per minute, and 10  $\mu$ L of each sample were injected into the column. All measurements were done at ambient temperature. Peak areas correlated linearly with the concentrations of gentiopicrin and oleanolic acid in the range of 5–400  $\mu$ g/mL.

## Pathologic observations on ELISA

Thirty Sprague-Dawley rats were randomized into five treatment groups to receive no treatment (blank controls), carbon

tetrachloride only (negative controls), gentiopicrin and normal saline, oleanolic acid and normal saline, or GO-NLCs. All rats were fasted for 12 hours before the experiments but had free access to water. A 25 mg/kg dose of the allocated treatment was injected intraperitoneally once a day for 12 days except in the blank and negative control groups, which were injected with isopyknic normal saline. Carbon tetrachloride was dissolved in 1 mL of olive oil at a ratio of 1:1 for administration on days 5, 8, and 12. Sixteen hours after the final injection of carbon tetrachloride, whole blood was collected and centrifuged at 3000 rpm for 10 minutes. Subsequent procedures were performed using an ELISA kit according to the manufacturer's instructions.<sup>22</sup>

After 20 minutes at room temperature, a slit was taken from the sealed foil for creation of sample and standard holes. Sample holes were added to test 10  $\mu$ L samples first, after which the diluent sample volume added was 40  $\mu$ L. Next, 50  $\mu$ L samples of standard solutions at different concentrations were added to the standard holes. One hole was left empty as the blank control. Next, 100  $\mu$ L of horseradish peroxidase-labeled antibody was added to each hole and the holes were then sealed with microplate sealers. The slit was incubated for one hour at 37°C in an incubator. The liquid was discarded and the samples were patted dry five times using filter paper. Each hole was coupled with 50  $\mu$ L each of substrate A and substrate B and incubated for 15 minutes while protected from light. Next, 50  $\mu$ L of stop solution was added to each hole. The optical densities of aspartate aminotransferase (AST) and alanine aminotransferase (ALT) were measured by ELISA (Anthos Labtec Instruments, Wals, Austria). Standard curves were constructed using the concentrations recommended in the ELISA kit. The enzyme activity in the samples was calculated using the regression equation for standard curves. Hepatic tissue specimens (5 mm  $\times$  5 mm  $\times$  3 mm) were taken from the same parts of the liver in each group and fixed in 10% neutral formaldehyde solution. The tissue specimens were then dehydrated in alcohol, embedded in paraffin, and cut into slices. Finally, pathologic sections were stained with hematoxylin and eosin, and observed under a microscope.

## Statistical analysis

The statistical analysis was performed using analysis of variance.  $P < 0.05$  was considered to be statistically significant. The data are presented as the mean  $\pm$  standard deviation.

## Results and discussion

### HPLC analysis

Standard curves for oleanolic acid and gentiopicrin were drawn, with the peak area as the vertical axis and the concentration of



oleanolic acid as the abscissa. The linear regression equation for oleanolic acid was  $y = 4977.7x + 189291$  and  $R^2 = 0.9997$  and for gentiopicrodin was  $y = 9864x + 63358$  and  $R^2 = 0.9993$ , indicating a good linear relationship between the peak areas and concentrations of both oleanolic acid and gentiopicrodin.

## Single effective factor experiments for GO-NLCs

A particle size study using the same concentrations of Poloxamer 188, Tween 80, Span 40, and polyvinylpyrrolidone was carried out first to select a suitable surfactant for the NLCs. When Poloxamer 188 was used as the surfactant during preparation of the NLCs, the particle size of the blank NLCs was about 150 nm and the absolute zeta potential was about 22 mV, as shown in Figure 1. The characterizations were fitting expectation, so Poloxamer 188 was chosen as the surfactant. The other factors were then determined, and samples containing Poloxamer 188 concentrations of 0.1%, 0.5%, 1%, 1.5%, and 2% were prepared. Taking into account the fact that particle size was probably less sensitive to changes in concentration, entrapment efficiency was investigated in this part of the experiment. As described in Figure 2, if the two drugs were considered collectively, the total entrapment efficiency of GO-NLCs was positively correlated with the Poloxamer 188 concentration. But the entrapment efficiency of

oleanolic acid was nearly 90% while that of gentiopicrodin was less than 10% when the concentration of Poloxamer 188 was 2%. In order to make the entrapment efficiency as balanced as possible, a Poloxamer 188 concentration of 1.5% was selected.

The influence of oleic acid on the particle size and entrapment efficiency of GO-NLCs was investigated, and the results are shown in Figure 3A. The entrapment efficiency of oleanolic acid increased significantly ( $P < 0.05$ ) when the concentration of oleic acid was increased from 10% to 50%. The entrapment efficiency of oleanolic acid reached a maximum when the proportion of oleic acid was 50%. The entrapment efficiency of gentiopicrodin was not so sensitive to an increase in oleic acid, and reached a maximum when the proportion of oleic acid was 40%. In these proportions, the entrapment efficiencies of gentiopicrodin and oleanolic acid were relatively balanced, and there are several possible explanations for this, as follows. As the proportion of oleic acid increases, the number of imperfect spaces in the lipid particle matrix increases and more drug molecules can be trapped therein. However, the lipid matrix might be destroyed when the proportion of oleic acid becomes excessive and drug entrapment efficiency decreases. Mean particle size had a negative relationship with the proportion of oleic acid, being less than 100 nm at an oleic acid content of more than 50%. When the proportion of oleic acid increases to more

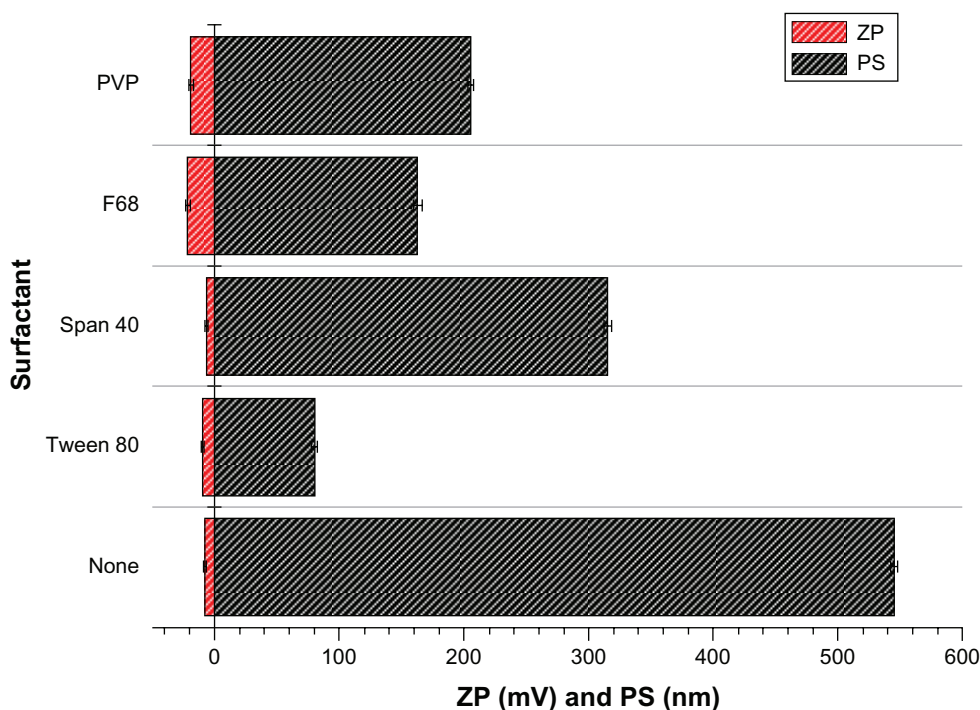


**Figure 1** Particle size and zeta potential of various surfactants.

**Abbreviations:** PS, particle size; ZP, zeta potential; PVP, polyvinylpyrrolidone.

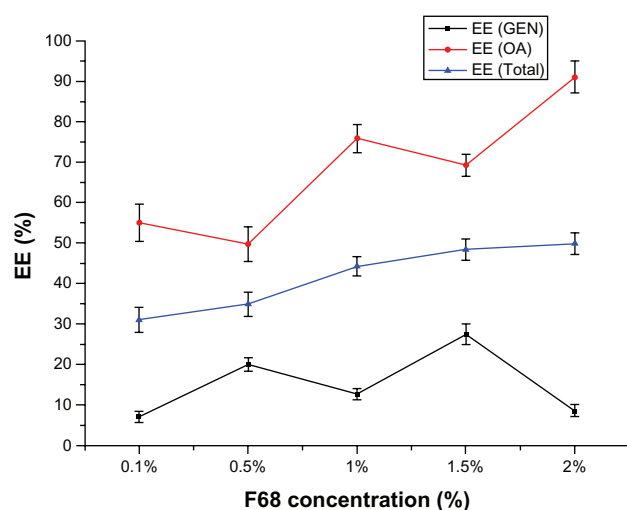


**Figure 2** Entrapment efficiency of samples prepared at different concentrations of Poloxamer 188.

**Abbreviations:** EE, entrapment efficiency; GEN, gentiopiricin; OA, oleanolic acid.

than 60%, particle size ceases to be sensitive to the proportion of oleic acid, as shown in Figure 3B.

Finally, the amount of drug as the single effective factor was studied. The entrapment efficiencies of oleanolic acid and gentiopiricin changed dramatically with changes in drug content. In contrast, there was only a slight change in particle size. It might be that space was limited in the imperfect lipid matrix, such that there was competition between the two drugs, indicating that the entrapment efficiency of gentiopiricin had a negative relationship with that of oleanolic acid. It was also found that the entrapment efficiencies of both gentiopiricin and oleanolic acid were highest at a drug content of about 3 mg. When designing novel formulations, it is important to identify factors influencing the properties of nanoparticles. Factors needing further optimization were identified to be the amounts of gentiopiricin, oleanolic acid, and oleic acid. Therefore, these three independent variables were used to design the experiments that followed.

## Optimization of formulations and statistical analysis

The results of the central composite design were analyzed using Design-Expert software, which provided useful information on parameters optimized by a limited number of experiments. From our earlier experiments, we knew that particle size was related to the surfactant used, duration of ultrasound exposure, and proportion of oleic acid included. After confirming Poloxamer 188 as the best surfactant, the ideal proportion of oleic acid to be 40%, and the optimal particle size range, the next parameter to

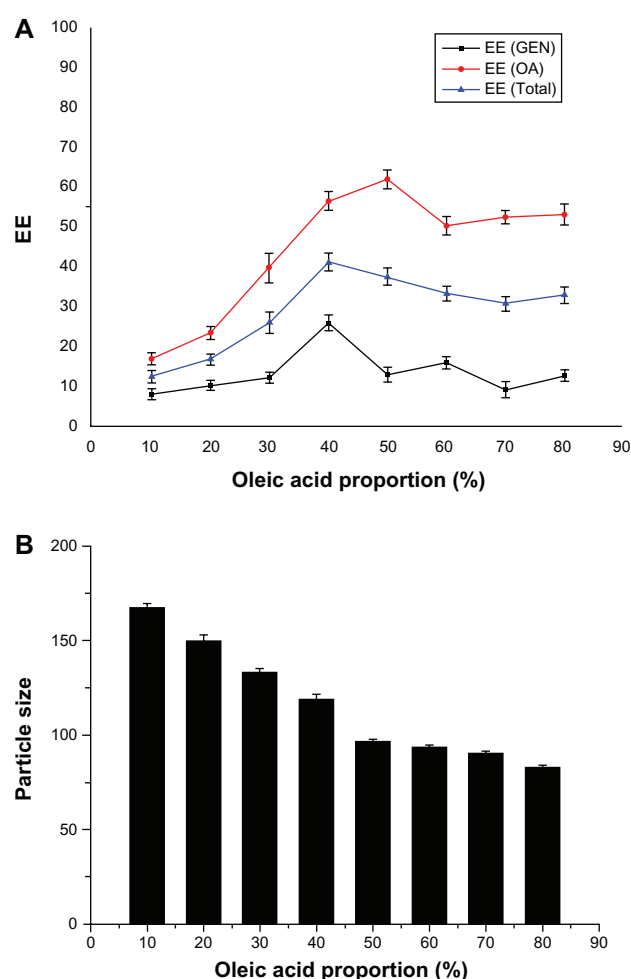


**Figure 3** Effect of proportion of oleic acid on drug entrapment efficiency (A) and particle size (B).

**Abbreviations:** EE, entrapment efficiency; GEN, gentiopiricin; OA, oleanolic acid.

be optimized was entrapment efficiency. The independent variables significantly influenced the responses observed with regard to percent entrapment efficiency for oleanolic acid, percent entrapment efficiency for gentiopiricin, and total entrapment efficiency.

The results of fitting the polynomial equation to the data for all three responses are shown in Table 3. The models was highly statistically significant ( $P < 0.01$ ), with a statistically insignificant lack of fit ( $P > 0.05$ ) for all responses. In addition, the amount of interaction between oleanolic acid and gentiopiricin was significantly ( $P < 0.01$ ) correlated with the entrapment efficiency of oleanolic acid and total entrapment efficiency, for which a three-dimensional map is shown in Figure 4. Other factors considered to be statistically insignificant ( $P > 0.05$ ) are not shown in Table 3. Therefore, mathematical models were used to describe the relationship between variables and responses.

**Table 3** Analysis of variance results for oleanolic acid, gentiopicrin and total entrapment efficiency, shown as R1, R2, and R3, respectively

	Source	Sum of squares	df	Mean square	F value	P value Probability > F
R1	Model	23.85	9	2.65	59.38	<0.0001
	A, oleanolic acid	1.71	1	1.71	38.25	0.0001
	C, oleic acid	0.74	1	0.74	16.48	0.0023
	AB	2.08	1	2.08	46.69	<0.0001
	A <sup>2</sup>	5.78	1	5.78	129.42	<0.0001
	B <sup>2</sup>	16.36	1	16.36	366.67	<0.0001
	C <sup>2</sup>	0.24	1	0.24	5.4	0.0424
	Residual	0.45	10	0.045		
	Lack of fit	0.45	5	0.089		
	Pure error	0.000	5	0.000		
	Cor total	24.30	19			
$y = 8.27 - 0.33x_1 - 0.043x_2 + 0.21x_3 - 0.51x_1x_2 - 1.690e - 0.003x_1x_3 - 0.024x_2x_3 - 0.48x_1^2 - 0.81x_2^2 - 0.098x_3^2 - 1.690e - 0.003x_1x_3 - 0.024x_2x_3 - 0.48x_1^2 - 0.81x_2^2 - 0.098x_3^2 - 1.690e - 0.003x_1x_3 - 0.024x_2x_3 - 0.48x_1^2 - 0.81x_2^2 - 0.098x_3^2$						
R2	Model	394.10	9	43.79	11.02	0.0004
	B, gentiopicrin	38.38	1	38.38	9.66	0.0111
	C <sup>2</sup>	321.59	1	321.59	80.96	<0.0001
	Residual	39.72	10	3.97		
	Lack of fit	39.72	5	7.94		
	Pure error	0.000	5	0.000		
	Total	433.82	19			
$y = 27.97 - 0.98x_1 - 1.55x_2 - 0.35x_3 + 0.97x_1x_2 - 0.090x_1x_3 + 0.08x_2x_3 - 0.48x_1^2 - 0.20x_2^2 - 3.58x_3^2$						
R3	Model	6.198E-003	9	6.887E-004	25.10	<0.0001
	B, gentiopicrin	5.904E-004	1	5.904E-004	21.52	0.0009
	C, oleic acid	1.490E-004	1	1.490E-004	5.43	0.0420
	AB	3.408E-004	1	3.408E-004	12.42	0.0055
	A <sup>2</sup>	1.887E-003	1	1.887E-003	68.77	<0.0001
	B <sup>2</sup>	4.107E-003	1	4.107E-003	149.68	<0.0001
	C <sup>2</sup>	5.688E-004	1	5.688E-004	20.73	0.0011
	Residual	2.744E-004	10	2.744E-005		
	Lack of fit	2.744E-004	5	5.487E-005		
	Pure error	0.000	5	0.000		
	Total	6.472E-003				
$y = 0.14 + 1.790e - 003x_1 + 6.075e - 003x_2 - 3.052e - 003x_3 + 6.526e - 003x_1x_2 - 2.917e - 004x_1x_3 + 1.034e - 003x_2x_3 + 8.663e - 003x_1^2 + 0.013x_2^2 + 4.756e - 003x_3^2$						

## Physicochemical characterization of GO-NLCs

Optimized GO-NLCs were prepared according to the formulation factors predicted by the central composite design. The average particle size and polydispersity index of the optimized GO-NLCs were  $111.0 \pm 1.56$  nm and  $0.287 \pm 0.01$  (Figure 5A), indicating that the NLCs were well distributed in the system. This particle size is suitable for use in nanomedicines. The zeta potential is also one of the important surface characteristics of GO-NLCs. As shown in Figure 5B, GO-NLCs had a mean zeta potential of  $-23.8 \pm 0.36$  mV. A suspension is deemed to be stable when the zeta potential is 30 mV, so the GO-NLCs created in this study were relatively stable.<sup>23</sup> Entrapment efficiency is the most important characteristic for estimating the

quality of NLCs. In general, the methods used to separate free drugs from NLCs are ultracentrifugation, a Sephadex column, and dialysis. A Sephadex column was used in the present study. There was a competitive relationship with regard to entrapment efficiency between the two components when they were loaded into the NLCs at the same time. This phenomenon could be explained by the different drug ingredients, ie, gentiopicrin (a hydrophilic molecule) and oleanolic acid (a hydrophobic molecule) being entrapped in one system with a steady drug-loading capacity. Therefore, there was a negative relationship between the entrapment efficiency of gentiopicrin and that of oleanolic acid. Finally, the optimized total entrapment efficiency and drug loading were  $48.34\% \pm 2.76\%$  and  $8.06 \pm 0.42$ , respectively.

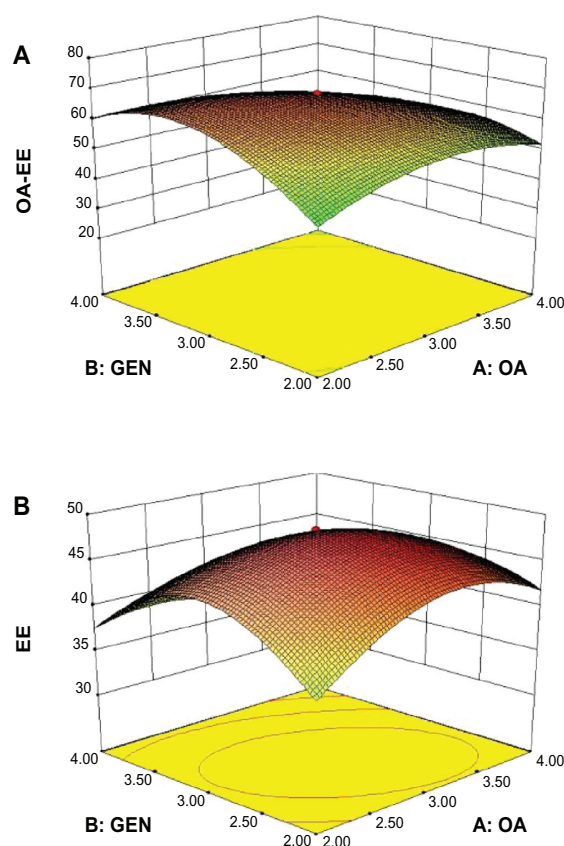


**Figure 4** Three-dimensional map of R1 (A) and R3 (B) follows interaction between independent variables (AB).

**Abbreviations:** EE, entrapment efficiency; GEN, gentiopiricin; OA, oleanolic acid.

Transmission electron microscopic imaging of the GO-NLCs (Figure 6) indicates that the particles were uniformly in the nanosize range and of spherical morphology. Differential scanning calorimetry was used to investigate the melting and crystallization behavior of the lipids

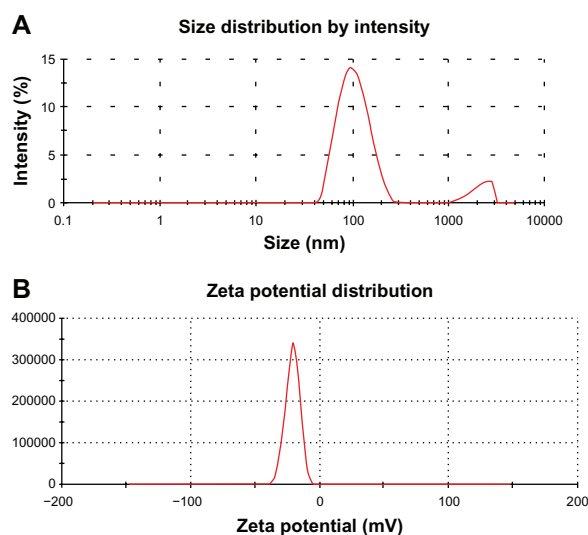


**Figure 5** Particle size distribution (A) and zeta potential distribution (B) of GO-NLCs.

**Abbreviation:** GO-NLCs, nanostructured lipid carriers loaded with both oleanolic acid and gentiopiricin.

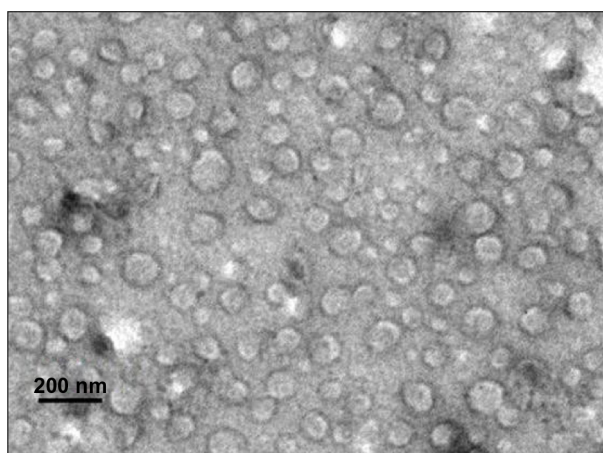


**Figure 6** Transmission electron microscopy of optimized nanostructured lipid carriers loaded with both oleanolic acid and gentiopiricin showing spherical morphology ( $\times 87,000$ ).

and NLCs. The melting point of the single solid lipid was higher than that of the mixed lipid; further, the melting range was shorter and the peak at higher temperature was narrower.<sup>24</sup> Figure 7 shows that endothermic peaks appeared at different degrees. Comparing the four curves for glycerin monostearate, gentiopiricin, oleanolic acid, and GO-NLCs, significant differences were observed, indicating that gentiopiricin and oleanolic acid were dispersed within the NLCs formed by glycerin monostearate and oleic acid. GO-NLCs showed no endothermic peaks for gentiopiricin and oleanolic acid, indicating that gentiopiricin and oleanolic acid existed in an amorphous state in the nanoparticles.

## In vitro release

Figure 8 shows the release profiles for gentiopiricin and oleanolic acid from GO-NLCs. Relative burst drug release was found for free gentiopiricin and oleanolic acid. In the contrast with the nonencapsulated drug formulations, there was a pronounced prolongation of drug release from the NLCs. While about 90% of the nonencapsulated drugs were found in the release medium, only 70% of the drugs were released from the nanoparticles after approximately 10 hours. The four release curves shown in Figure 8 indicate that oleanolic acid was released more slowly than gentiopiricin from GO-NLCs, perhaps because of the hydrophobicity of oleanolic acid. The cumulative amount of oleanolic acid loaded into the GO-NLCs was slightly less than that of gentiopiricin at almost any time point. Cumulative release data for the optimized GO-NLCs were used to fit zero-order, first-order and Higuchi equations, as shown in Table 4. Release of gentiopiricin and oleanolic acid from GO-NLCs



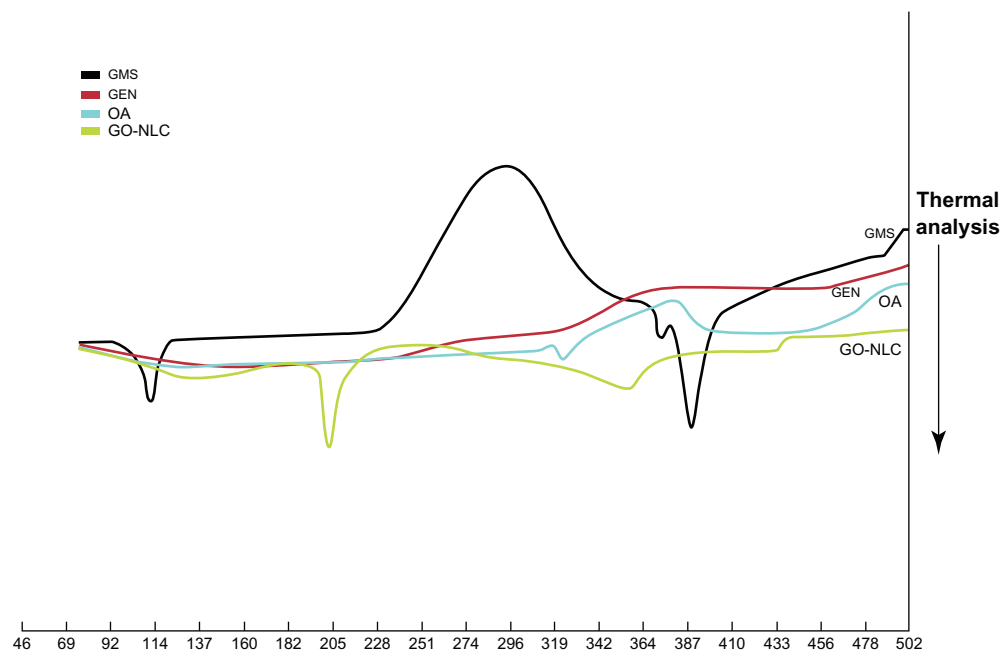


**Figure 7** Differential scanning calorimetry curve of GMS, GEN, OA, and freeze-dried GO-NLCs.

**Abbreviations:** GMS, glycerin monostearate; GEN, gentiopiricin; OA, oleanolic acid; GO-NLCs, nanostructured lipid carriers loaded with both oleanolic acid and gentiopiricin.

fitted a sustained-release first-order model, the mechanism for which might be explained by the fact that most of the liquid lipid was distributed in the solid lipid core, and the drug incorporated into the solid-liquid lipid matrix was released in a sustained manner via erosion or degradation.<sup>25</sup>

## Pharmacokinetic studies

The standard curves for gentiopiricin and oleanolic acid were  $y = 971.51x + 51365$  and  $y = 1844x + 63675$ , respectively, and within the concentration range of 0.3–100  $\mu\text{g/mL}$ , showed good linearity with correlation coefficients of 0.9988 and

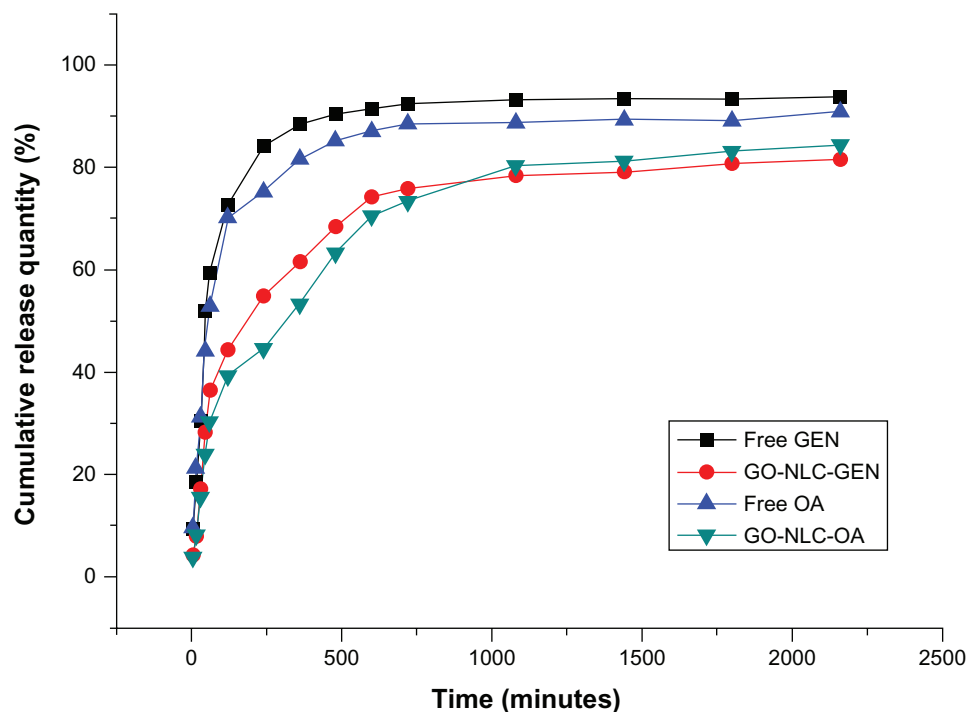


**Figure 8** In vitro release curves for GEN, OA, and GO-NLCs.

**Abbreviations:** GEN, gentiopiricin; OA, oleanolic acid; GO-NLCs, nanostructured lipid carriers loaded with both oleanolic acid and gentiopiricin.

**Table 4** Models for drug-release fitting and correlation coefficients of nanostructured lipid carriers loaded with both oleanolic acid and gentiopiricin

Model	Equation	R <sup>2</sup>
Gentiopiricin		
Zero-order	$y = 0.031x + 34.131$	0.6035
First-order	$y = 14.743 \ln(x) - 25.938$	0.9745
Higuchi	$y = 3.4661x^{0.4606}$	0.8872
Oleanolic acid		
Zero-order	$y = 0.0347x + 29.354$	0.7057
First-order	$y = 15.257 \ln(x) - 31.173$	0.9706
Higuchi	$y = 2.8874x^{0.4818}$	0.9305

0.9998, respectively. The blood concentration-time profiles for the drugs and GO-NLCs are shown in Figure 9, and fit a two-compartment model. As seen in Figure 9, the initial drug concentrations of gentiopiricin and oleanolic acid were higher than that of the GO-NLCs; however, gentiopiricin and oleanolic acid were rapidly removed from the circulation in comparison with the GO-NLC formulation. In addition, elimination of the GO-NLCs was slower than that for gentiopiricin or oleanolic acid. The mean values of the main pharmacokinetic parameters for gentiopiricin, oleanolic acid, and GO-NLCs are shown in Table 5. The area under the concentration-time curve for GO-NLCs was greater than that for gentiopiricin or oleanolic acid. Specifically, the area under the curve for the GO-NLC

group was 1.57 and 1.44 times that of the oleanolic acid group and gentiopiricin group, respectively, indicating that the absorption of gentiopiricin and oleanolic acid was significantly increased. The significant difference in alpha elimination half-life between the groups indicated that the distribution of GO-NLCs was less than that of oleanolic acid or gentiopiricin. The significant difference in beta elimination half-life and clearance indicates that the elimination of GO-NLCs was slower and that the circulation time was longer.

## Pathologic observations on ELISA

Because of its feasibility, accuracy, and high reliability, we chose the carbon tetrachloride model of acute liver injury in the rat for our experiments. Compared with controls, ALT and AST were significantly elevated in rats exposed to carbon tetrachloride, indicating that this model of acute liver damage was successful. Compared with carbon tetrachloride, ALT and AST of GO-NLCs significantly reduced ( $P < 0.05$ ), so did compared with gentiopiricin group and oleanolic acid group (Figure 10). ALT is mainly distributed in the cytoplasm of liver cells, and its value doubles with every 1% increase in liver cell necrosis. Therefore, ALT is recommended by the World Health Organization as a sensitive marker of liver damage. AST is distributed within the mitochondria of liver cells, and elevations of both ALT and

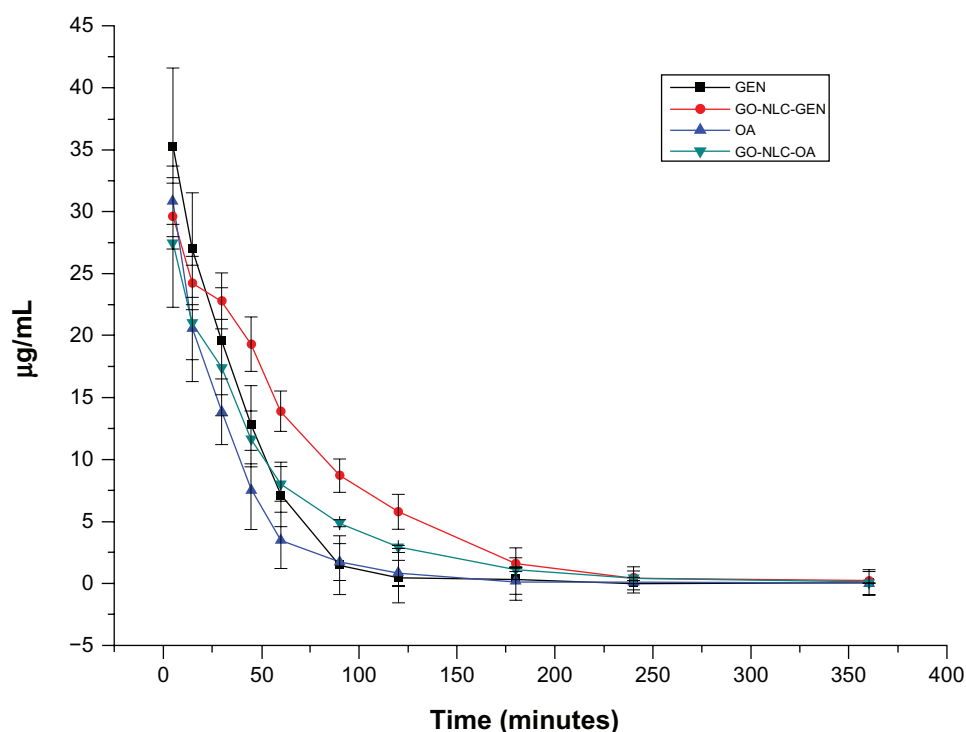


**Figure 9** Plasma concentration-time curves for gentiopiricin and oleanolic acid after intravenous administration of gentiopiricin + normal saline, oleanolic acid + normal saline, and nanostructured lipid carriers loaded with both oleanolic acid and gentiopiricin.

**Abbreviations:** GEN, gentiopiricin; OA, oleanolic acid; GO-NLCs, nanostructured lipid carriers loaded with both oleanolic acid and gentiopiricin.

**Table 5** Plasma pharmacokinetic parameters for gentiopiricin and oleanolic acid after intravenous administration of gentiopiricin, oleanolic acid, and GO-NLCs

Parameter	Unit	Gentiopiricin + NS	GO-NLCs Gentiopiricin	Oleanolic acid + NS	GO-NLCs Oleanolic acid
AUC	$\mu\text{g} \cdot \text{min} \cdot \text{mL}^{-1}$	$1370.400 \pm 21.947^{**}$	$2155.428 \pm 34.349^{**}$	$1052.806 \pm 16.613^{**}$	$1520.754 \pm 25.355^{**}$
A	$\mu\text{g/mL}$	$51.934 \pm 0.104^{**}$	$37.816 \pm 0.469^{**}$	$34.232 \pm 0.574^{**}$	$7.745 \pm 0.431^{**}$
alpha	minutes	$0.040 \pm 0.004^*$	$0.018 \pm 0.002^{**}$	$0.045 \pm 0.007^{**}$	$0.038 \pm 0.003^*$
B	$\mu\text{g/mL}$	$0.427 \pm 0.041^{**}$	$0.297 \pm 0.084^{**}$	$4.874 \pm 0.130^{**}$	$22.899 \pm 0.451^{**}$
beta	minutes	$0.005 \pm 0.003$	$0.004 \pm 0.001$	$0.017 \pm 0.001$	$0.017 \pm 0.001$
V (c)	$\text{mg} \cdot \text{mL} \cdot \mu\text{g/kg}$	$0.191 \pm 0.052^{**}$	$0.262 \pm 0.076^{**}$	$0.255 \pm 0.034^{**}$	$0.326 \pm 0.052^{**}$
$t_{1/2 \alpha}$	minutes	$17.157 \pm 0.273^{**}$	$38.115 \pm 0.432^{**}$	$15.529 \pm 0.393^{**}$	$18.164 \pm 0.775^{**}$
$t_{1/2 \beta}$	minutes	$137.814 \pm 1.864^{**}$	$177.516 \pm 2.244^{**}$	$40.658 \pm 0.897^{**}$	$39.890 \pm 0.821^{**}$
CL	$\text{mg} \cdot \text{min} \cdot \text{mL} \cdot \mu\text{g/kg}$	$0.007 \pm 0.001$	$0.005 \pm 0.001^*$	$0.010 \pm 0.001^*$	$0.007 \pm 0.001$

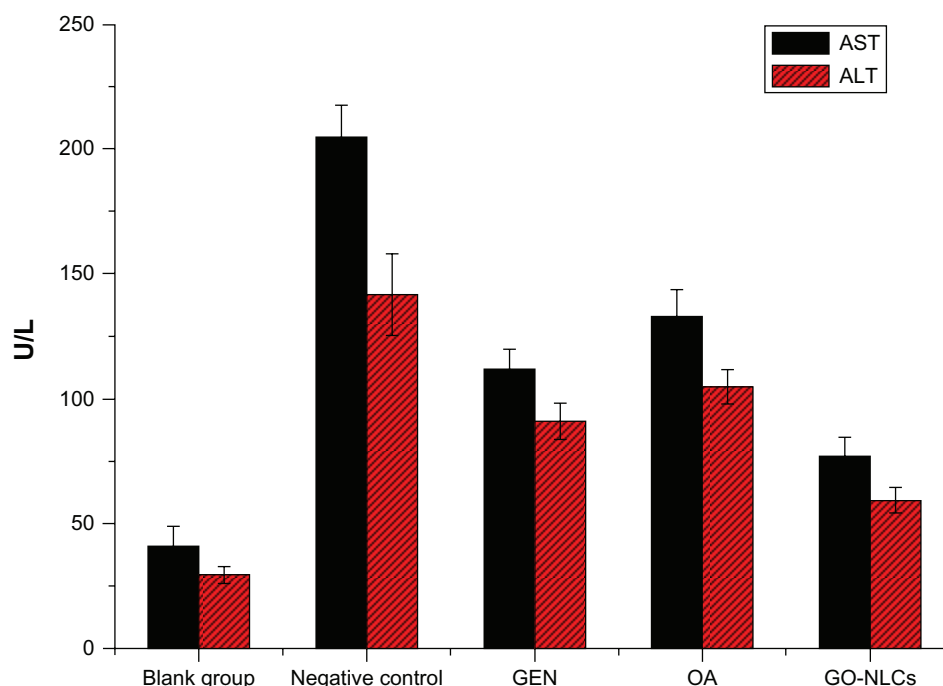
**Notes:** \* $P < 0.05$ ; \*\* $P < 0.01$ .

**Abbreviations:** AUC, area under the concentration-time curve; NS, normal saline; GO-NLCs, nanostructured lipid carriers loaded with both oleanolic acid and gentiopiricin; CL, clearance;  $t_{1/2 \alpha}$ , alpha elimination half-life;  $t_{1/2 \beta}$ , beta elimination half-life.

AST tend to be consistent with the degree of liver damage, so ALT and AST are the most commonly used indicators of liver function, although other diseases may also trigger elevation of ALT and AST. Because of the different distributions of ALT and AST in the liver, differences in ALT and AST levels and in the AST to ALT ratio indicate that the extent of hepatitis in patients is not always the same. Although there is damage to liver cells in acute, chronic, and mild hepatitis, the mitochondria with the liver cells remain intact. At this stage, ALT is released into the circulation only in the cytoplasm of liver cells. Therefore, elevated ALT plays an important role in determining liver function, and in our study, the AST/ALT ratio was less than 1. The mitochondria

are destroyed in severe hepatitis and chronic hepatitis, in which case AST are released from the mitochondria and the AST to ALT ratio is  $\geq 1$ . Therefore, ALT and AST are used to indicate the degree of liver damage.

The hepatic lobule was structurally intact in the control group, showing mild inflammatory cell infiltrates and regularly formed hepatocytes (Figure 11A). In the carbon tetrachloride liver injury model, there was swelling of hepatocytes, cytoplasmic laxity, infiltration by lymphocytes, inflammation, and fatty degeneration (Figure 11B). The hepatocytes treated with GO-NLCs were mildly disordered, with slight fatty degeneration and less infiltration by inflammatory cells (Figure 11C).

**Figure 10** Aspartate and alanine aminotransferase levels in rats suffering acute hepatic damage in response to administration of carbon tetrachloride.

**Abbreviations:** GEN, gentiopiricin; OA, oleanolic acid; GO-NLCs, nanostructured lipid carriers loaded with both oleanolic acid and gentiopiricin; AST, aspartate aminotransferase; ALT, alanine aminotransferase.

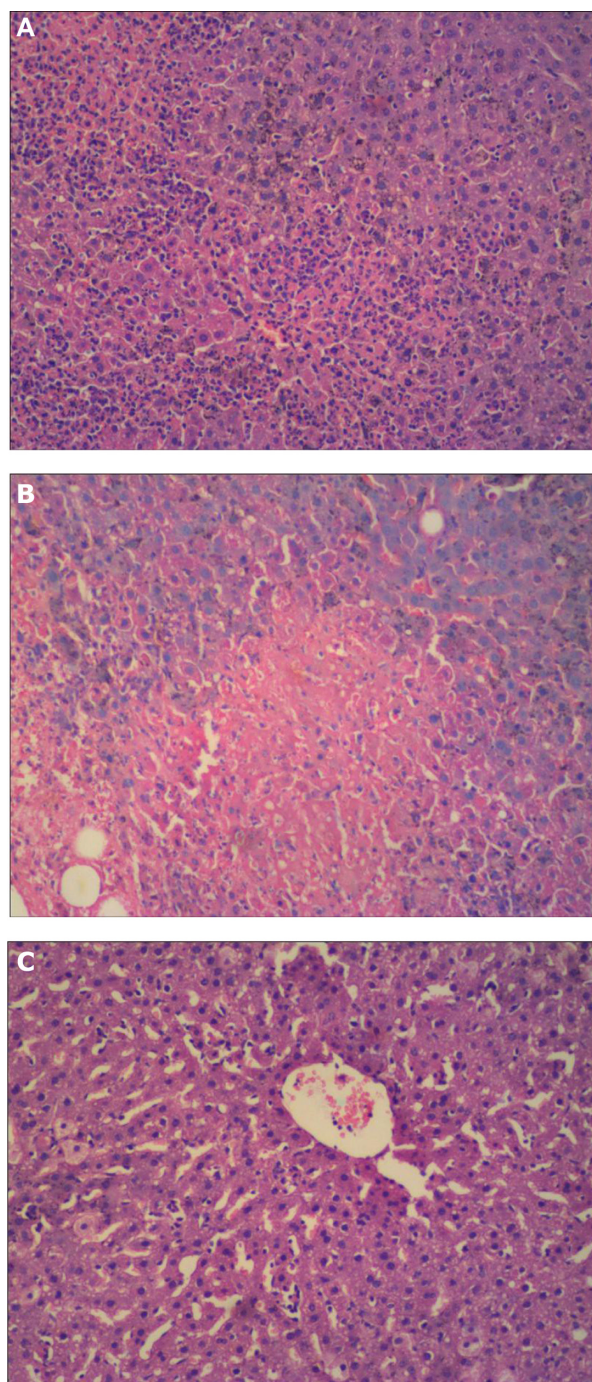


**Figure 11** Pathological observation of acute hepatic damage caused by carbon tetrachloride in the rat. (A) Control group, (B) carbon tetrachloride group, and (C) and group treated with nanostructured lipid carriers loaded with both oleanolic acid and gentiopicrocin.

## Conclusion

In this study, the influence of various processing parameters on particle size and drug entrapment efficiency were systematically addressed. A number of formulation variables could be regulated to improve the incorporation of gentiopicrocin and oleanolic acid into NLCs. GO-NLCs

were successfully prepared using the film-ultrasonic method and optimized by a central composite design. Using the optimized parameters, it was possible to formulate GO-NLCs with predictable characteristics. To the authors knowledge, this is the first report of two drugs with different properties being simultaneously entrapped into NLCs. The oleic acid ratio was an important factor with regard to both entrapment efficiency and particle size. The concentration of the surfactant (Poloxamer 188) and the amount of drug incorporated were also crucial factors determining drug entrapment efficiency, but did not influence particle size. Our study results indicate that models with a central composite design are highly statistically significant. The physicochemical properties of the GO-NLCs constructed in this study were characterized in detail, with in vitro drug release patterns showing relatively prolonged drug release. Pharmacokinetic studies demonstrated that the half-life and residence time of the GO-NLCs in vivo were significantly prolonged. Because of the significant changes in these pharmacokinetic parameters, GO-NLCs have the potential to improve the bioavailability of oleanolic acid and gentiopicrocin and have a sustained-release effect. GO-NLCs also reversed elevations of ALT and AST in a rat model of acute hepatic damage induced by carbon tetrachloride. In summary, our findings may promote the development of NLCs loaded simultaneously with drugs having different characteristics. GO-NLCs could be a promising formulation for prolonging drug circulation times in blood.

## Acknowledgments

The authors are grateful for the grants received in support of this research from the Technology Division Foundation of Haerbin (2012 RF XXS003) and the National Natural Science Foundation of China (81274091).

## Disclosure

The authors report no conflicts of interest in this work.

## References

1. Kondo Y, Takano F, Hojo H. Suppression of chemically and immunologically induced hepatic injuries by gentiopicrosin in mice. *Planta Med.* 1994;60:414–416.
2. Liu YP, Hartley PD, Liu J. Protection against carbon tetrachloride hepatotoxicity by oleanolic acid is not mediated through metallothionein. *Toxicol Lett.* 1998;95:77–85.
3. Jeong HG. Inhibition of cytochrome P450 2E1 expression by oleanolic acid: hepatoprotective effects against carbon tetrachloride-induced hepatic injury. *Toxicol Lett.* 1999;105:215–222.
4. Wang MT, Jin Y, Yang YX, et al. In vivo biodistribution, anti-inflammatory, and hepatoprotective effects of liver targeting dexa-methasone acetate loaded nanostructured lipid carrier system. *Int J Nanomedicine.* 2010;5:487–497.



5. Müller RH, Radtke M, Wissing SA. Solid lipid nanoparticles (SLN) and nanostructured lipid carriers (NLC) in cosmetic and dermatological preparations. *Adv Drug Deliv Rev.* 2002;54:131–155.
6. Müller RH, Radtke M, Wissing SA. Nanostructured lipid matrices for improved microencapsulation of drugs. *Int J Pharm.* 2002;242:121–128.
7. Das S, Chaudhury A. Recent advances in lipid nanoparticle formulations with solid matrix for oral drug delivery. *AAPS Pharm Sci Tech.* 2011;12:62–76.
8. Luo QH, Zhao JM, Zhang XR, et al. Nanostructured lipid carrier (NLC) coated with chitosan oligosaccharides and its potential use in ocular drug delivery system. *Int J Pharm.* 2011;403:185–191.
9. Shah P, Desai P, Channer D, et al. Enhanced skin permeation using polyarginine modified nanostructured lipid carriers. *J Control Release.* 2012;161:735–746.
10. Jia LJ, Shen JY, Zhang DR, et al. In vitro and in vivo evaluation of oridonin-loaded long circulating nanostructured lipid carriers. *Int J Biol Macromol.* 2012;50:523–529.
11. Eskandari S, Varshosaz J, Minaian M, et al. Brain delivery of valproic acid via intranasal administration of nanostructured lipid carriers: in vivo pharmacodynamic studies using rat electroshock model. *Int J Nanomedicine.* 2011;6:363–371.
12. Guo CY, Yang CF, Li QL, et al. Development of a quercetin-loaded nanostructured lipid carrier formulation for topical delivery. *Int J Pharm.* 2012;430:292–299.
13. Fang JY, Fang CL, Liu CH, et al. Lipid nanoparticles as vehicles for topical psoralen delivery: solid lipid nanoparticles (SLN) versus nanostructured lipid carriers (NLC). *Eur J Pharm Biopharm.* 2008;70:633–640.
14. Blasi P, Giovagnoli S, Schoubben A, et al. Solid lipid nanoparticles for targeted brain drug delivery. *Adv Drug Deliv Rev.* 2007;59:454–477.
15. Löbenberg R, Maas J, Kreuter J. Improved body distribution of 14C-labelled AZT bound to nanoparticles in rats determined by radioluminography. *J Drug Target.* 1998;5:171–179.
16. Sawant RR, Vaze SO, Rockwell K, et al. Palmitoyl ascorbate-modified liposomes as nanoparticle platform for ascorbate-mediated cytotoxicity and paclitaxel codelivery. *Eur J Pharm Biopharm.* 2010;75:321–326.
17. Shi F, Zhao JH, Liu Y, et al. Preparation and characterization of solid lipid nanoparticles loaded with frankincense and myrrh oil. *Int J Nanomedicine.* 2012;7:2033–2043.
18. Gokce HE, Korkmaz E, Dellera E, et al. Resveratrol-loaded solid lipid nanoparticles versus nanostructured lipid carriers: evaluation of antioxidant potential for dermal applications. *Int J Nanomedicine.* 2012;7:1841–1850.
19. Gao DW, Tang SN, Tong Q. Oleanolic acid liposomes with polyethylene glycol modification: promising antitumor drug delivery. *Int J Nanomedicine.* 2012;7:3517–3526.
20. Elnaggar SY, El-Massik AM, Abdallah YO. Fabrication, appraisal, and transdermal permeation of sildenafil citrate-loaded nanostructured lipid carriers versus solid lipid nanoparticles. *Int J Nanomedicine.* 2011;6:3195–3205.
21. Chen CC, Tsai TH, Huang ZR, et al. Effects of lipophilic emulsifiers on the oral administration of lovastatin from nanostructured lipid carriers: physicochemical characterization and pharmacokinetics. *Eur J Pharm Biopharm.* 2010;74:474–482.
22. Murakami K, Takahashi R, Ono M, et al. Serodiagnosis of *Helicobacter hepaticus* infection in patients with liver and gastrointestinal diseases: western blot analysis and ELISA using a highly specific monoclonal antibody for *H. hepaticus* antigen. *J Gastroenterol.* 2011;46:1120–1126.
23. Brgles M, Jurašin D, Sikirić DM, et al. Entrapment of ovalbumin into liposomes – factors affecting entrapment efficiency, liposome size, and zeta potential. *J Lipid Res.* 2008;18:235–248.
24. Castelli F, Puglia C, Sarpietro GM, et al. Characterization of indomethacin-loaded lipid nanoparticles by differential scanning calorimetry. *Int J Pharm.* 2005;304:231–238.
25. Pardeike J, Weber S, Matsko N, et al. Formation of a physical stable delivery system by simply autoclaving nanostructured lipid carriers (NLC). *Int J Pharm.* 2012;439:22–27.

## International Journal of Nanomedicine

### Publish your work in this journal

The International Journal of Nanomedicine is an international, peer-reviewed journal focusing on the application of nanotechnology in diagnostics, therapeutics, and drug delivery systems throughout the biomedical field. This journal is indexed on PubMed Central, MedLine, CAS, SciSearch®, Current Contents®/Clinical Medicine,

Submit your manuscript here: <http://www.dovepress.com/international-journal-of-nanomedicine-journal>

Dovepress

Journal Citation Reports/Science Edition, EMBase, Scopus and the Elsevier Bibliographic databases. The manuscript management system is completely online and includes a very quick and fair peer-review system, which is all easy to use. Visit <http://www.dovepress.com/testimonials.php> to read real quotes from published authors.